Kontrast Ajan Iopromidinin Elektronik Yapısı Üzerine Teorik B3LYP Çalışması

Giray Sedat KANDEMİRLİ[2], M. İzzettin YILMAZER [1]*,
Fatma KANDEMİRLİ[3], Murat SARAÇOĞLU[4]

*[1] Erciyes University, Faculty of Education Educational Sciences, KAYSERI
[2] University of Lowa, Roy Carver College of Medicine, Department of Radiology, UNITED STATES
[3]Kastamonu University, Faculty of Engineering and Architecture, Biomedical Engineering Department, KASTAMONU
[4]Erciyes University, Faculty of Education, Mathematics and Science Education, KAYSERI

(Alınış / Received: 27.01.2020, Kabul / Accepted: 04.08.2020, Online Yayınlanma / Published Online: 31.12.2020)

Anahtar Kelimeler
İyopromidin,
DFT,
B3LYP,
Kuantum kimyasal hesaplamalar.

Öz: İyopromidinin moleküler yapısı, B3LYP/CEP-121G ve PBE/TZP seviyelerinde DFT hesaplamaları ile belirlenmiştir. İyoprimidinin bileşiğinin gaz fazı ve farklı çözücülerde örnek olarak, kloroform, asetik asit, etanol, DMF, DMSO, su, elektronik, yapısal ve termodinamik özellikleri, manyetik momenti, statik ve dinamik polarizasyonu (α ve Δα) ve hiperpolarizasyon kabiliyeti (β, γ), B3LYP yönteminin CEP-4G, CEP-31G, CEP-121G, DGDZVP ve LANL2DZ baz setleri kullanılarak Gaussian 09 yazılımı yardımıyla belirlenmiştir. Zamana bağlı yoğunluk fonksiyonel teorisi (TD-DFT) ile gaz fazında ve farklı çözücülerdeki iyopromidinin optik absorpsiyon spektrumunu hesaplamak için de kullanılmıştır.

Theoretical B3LYP Study on Electronic Structure of Contrast Agent Iopromide

Keywords
Iopromide,
DFT,
B3LYP,
Quantum chemical calculations.

Abstract: The molecular structure of iopromide was determined by DFT calculations at B3LYP/CEP-121G and PBE/TZP levels. Electronic, structural, and thermodynamic properties, magnetic moment, static and dynamic polarizability (α and $\Delta\alpha$) and hyperpolarizability (β, γ) of iopromide compound were determined by using B3LYP method with the CEP-4G, CEP-31G, CEP-121G, DGDZVP and LANL2DZ basis sets in gas phase and different solvents such as chloroform, acetic acid, ethanol, DMF, DMSO, water with the assistance of Gaussian 09 software. The effect of solvent on parameters has been studied. Time dependent density functional theory (TD-DFT) has also been used to calculate the optical absorption spectrum of iopromide in gas phase and in different solvents.

*İlgili Yazar, email: izzettin@erciyes.edu.tr

1. Introduction

Iodinated X-ray contrast media are sterile iodine-containing solutions and they are the most commonly used drugs in diagnostic and interventional procedures. Contrast media which are categorised as ionicmonomers, ionic dimers, nonionic monomers and nonionic dimers differ due to in their osmolality, number of hydroxyl and carboxyl groups [1]. Iodinated contrast media non-ionic monomers, such as iohexol, iopamidol, iomeprol, iopromide, and ioversol have been commercially marketed for long periods, and their safety has been confirmed clinically [2-4] determined the characteristic AEs of iodinated contrast media and to compare the safety profiles of different iodinated contrast media using data from spontaneous post-marketing and reported that Iopromide (45.5%) was the most commonly implicated iodinated contrast medium, followed by iohexol (16.9%), iopamidol (14.3%) and iomeprol (10.3%). Iopromide is a dicarboxylic acid diamide that consists of N-methylisophthalamide bearing three iodo substituents at positions 2, 4 and 6 a methoxyacetyl substituent at position 5 and two 2,3-dihydroxypropyl groups attached to the amide nitrogens.

Starry [5] synthesized iopromide from 3-amino-5-(2,3-diacetoxypropylcarbamoyl)-2,4,6-triiodobenzoic acid by reaction with methoxyacetyl chloride, hydrolysis with $NaHCO_3$ and chlorination to give 3-(2-methoxyacetylamino)-5-(2,3-dihydroxypropylcarbamoyl)-2,4,6-triiodobenzoyl chloride, followed by reaction with N-methyl-2,3-dihydroxypropylamine with an overall yield of about 80%.

In internal organ examinations where the difference in X-ray absorption between the organ and adjacent tissues is small, therefore contrast agents with different absorption rates are used to increase the difference in X-ray absorption. There are two types of contrast media, i.e. positive contrast agents that absorb the X-ray well and negative contrast agents that transmit the X-ray well and a suitable type is used for the purpose of examination.

In this research work, HOMO and LUMO energies, parameters related with HOMO and LUMO energies molecular polarizability (α) and first hyperpolarizabilities, thermodynamic properties are calculated using B3LYP level using by the DFT level and B3LYP functionals with the CEP-4G, CEP-121G, CEP-31G, DGDZVP and LANL2DZ basis sets iopromide molecule for gas and solvent media such chloroform, acetic acid, ethanol, DMF, DMSO and water using Gaussian 09, Revision A.02 program [6].

2. Computation Methods

The input files of the complex were prepared with GaussView 5.0.8 [7]. Calculations were made using Gaussian 09, Revision A.02 program [6]. Quantum chemical properties of iopromide were determined through the application of density functional theory (DFT) methods (B3LYP) [8], with LANL2DZ [9], CEP-4G [10], CEP-31G [11] and CEP-121G [11] basis sets.

2.1. Computational details

In this study, all calculations were carried out by using DFT/B3LYP method. Optimization of synthesized molecules was performed with 6-311G(d,p) basis set of Gaussian 09, Revision A.02 program [6]. Quantum chemical parameters for synthesized molecules such as; the energy of the highest occupied molecular orbital (E_{HOMO}), the energy of the lowest unoccupied molecular orbital (E_{LUMO}), HOMO-LUMO energy gap (ΔE), ionization energy (I), chemical hardness (η), softness (σ), electronegativity (χ), chemical potential (μ), dipole moment (DM), global electrophilicity (ω) and sum of negative Mulliken atomic charges (MAC), summary of natural population analysis (SNPA) for gas and different phases of neutral molecules were calculated and discussed. Recently, the optimization of the molecules with different basic groups and the discussion of the results have been widely used [12-33].

Molecular properties, related to the reactivity and selectivity of the compounds, were estimated following the Koopmans's theorem [34] relating the energy of the HOMO and the LUMO. According to the DFT-Koopmans' theorem [34, 35], the ionization potential (I) can be approximated as the negative value of the highest occupied molecular orbital energy (E_{HOMO}), such as shown in equation 1:

$$I = -E_{HOMO} \tag{1}$$

The negative value of the lowest unoccupied molecular orbital energy (E_{LUMO}) is similarly related to the electron affinity (A) [36] shown in equation 2:

$$A = -E_{LUMO} \tag{2}$$

Energy gap (ΔE) is estimated by using the E_{HOMO} and E_{LUMO}:

$$\Delta E = E_{LUMO} - E_{HOMO} \tag{3}$$

Electronegativity (χ) is estimated with the following the equation from E_{HOMO} and E_{LUMO} [37] or ionization potential (I) and electron affinity (A) [38]:

$$\chi \cong -\left(\frac{E_{HOMO} + E_{LUMO}}{2}\right) = \left(\frac{I + A}{2}\right) \tag{4}$$

Chemical hardness (η) measures the resistance of an atom to a charge transfer [37], it's estimated by using the equation 5 from E_{HOMO} and E_{LUMO} or I and A [38]:

$$\eta \cong -\left(\frac{E_{HOMO} - E_{LUMO}}{2}\right) = \left(\frac{I - A}{2}\right) \tag{5}$$

Electron polarizability, called chemical softness (σ), describes the capacity of an atom or group of atoms to receive electrons [37], and it is estimated by using the equation 6:

$$\sigma = \frac{1}{\eta} \cong -\left(\frac{2}{E_{HOMO} - E_{LUMO}} \right) \tag{6}$$

Chemical potential (μ) and electronegativity (χ) can be calculated with the help of the following equation [12] from E_{HOMO} and E_{LUMO}:

$$\mu = -\chi \cong \left(\frac{E_{HOMO} + E_{LUMO}}{2} \right) \tag{7}$$

The global electrophilicity index (ω) is a useful reactivity descriptor that can be used to compare the electron-donating abilities of molecules [39]. Global electrophilicity index is estimated by using the electronegativity (χ) and chemical hardness (η) parameters through the equation:

$$\omega = \frac{\chi^2}{2\eta} \tag{8}$$

A high value of electrophilicity describes a good electrophile while a small value of electrophilicity describes a good nucleophile [40].

3. Result and Discussion

The most important orbital in the molecule is the so-called frontier orbitals known as HOMO and LUMO. LUMO the lowest unoccupied molecular orbital HOMO is the highest energy MO. The optimized structure and, the pictorial representation of their HOMO-LUMO distribution and their respective positive and negative regions of mentioned molecule at B3LYP/LANL2DZ level for gas phase are shown in **Figure 1**.

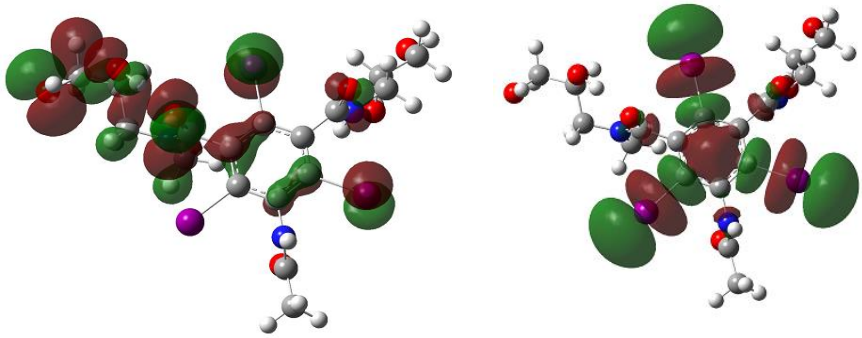

HOMO LUMO

Figure 1. The frontier MOs (HOMOs, LUMOs) of molecules by using DFT/B3LYP/LANL2DZ basic set.

As seen from **Figure 1**, both HOMO and LUMO plots simulated with B3LYP/LANL2DZ level were localized on the groups attached to **C16** atom of benzyl group for iopromide molecule. Green and red colour represents the positive and negative phase, respectively of the iopromide molecule.

The highest occupied molecular orbital (HOMO) that represents the ability to donate an electron and the lowest unoccupied molecular orbital (LUMO) as an electron acceptor that obtains electron are the main orbitals that take part in chemical stability. Energy gap that is difference between HOMO and LUMO energy is an important stability for molecules [41]. E_{HOMO}, E_{LUMO} and ΔE of iopromide molecule calculated by the DFT level and B3LYP functionals with the CEP-4G, CEP-121G, CEP-31G, DGDZVP and LANL2DZ basis sets in gas, chloroform, acetic acid, ethanol, DMF, DMSO and water phases are presented in **Figures 2-4**.

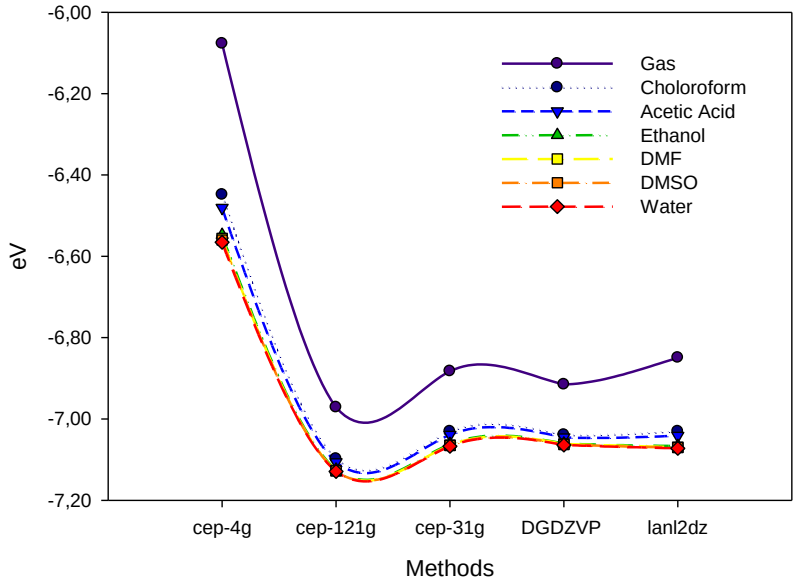

Figure 2. The calculated HOMO parameters by using CEP-4G, CEP-121G, CEP-31G, DGDZVP and LANL2DZ basis sets in gas, chloroform, acetic acid, ethanol, DMF, DMSO and water phases.

As seen from the **Figure 2**, we can say that HOMO energy on going from the gas phase to water phase for all the bases set decreased by solvent dielectric constant for all the studied basis sets. The HOMO energy of iopromide molecule have deceased in the following order: -6.849 eV in gas phase > -7.030 eV in chloroform > -7.041 eV in acetic acid > -7.067 eV in ethanol > -7.069 eV in DMF > -7.070 eV in DMSO > -7.072 in water at LANL2DZ basis set. According to these results, the electron donating trends for study molecule for different phase can be written for LANL2DZ basis set as: gas phase < chloroform < acetic acid < ethanol < DMF < DMSO < water. However, LUMO energy on going from the gas phase to solvent phase at LANL2DZ basis set slightly increased from -2.2893 eV to -2.2850 eV in chloroform and then decreased as the dielectric constant of the solvent increased. The similar trend is seen for DGDZVP basis set (**Figure 3**).

The largest HOMO-LUMO energy gap (ΔE) was found in water solvent for the all studied basis set which implies higher kinetic stability and less chemical reactivity [42] and the smallest ΔE was found in gas phase for the all studied basis set. The ΔE of iopromide molecule have deceased in the following order: 4.560 eV in gas phase < 4.745 eV in chloroform < 4.755 eV in acetic acid < 4.777 eV in ethanol < 4.779 eV in DMF < 4.781 eV in DMSO < 4.782 eV in water at LANL2DZ basis set; 4.614 eV in gas phase < 4.757 eV in chloroform < 4.763 eV in acetic acid < 4.776 eV in ethanol < 4.776 eV in DMF < 4.778 eV in DMSO < 4.778 eV in water at DGDVZ basis set (**Figure 4**).

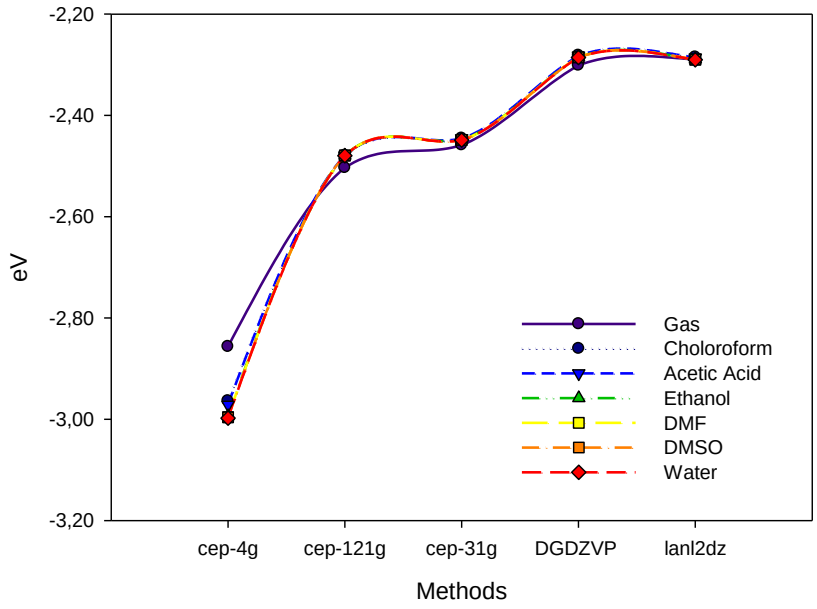

Figure 3. The calculated LUMO parameters by using CEP-4G, CEP-121G, CEP-31G, DGDZVP and LANL2DZ basis sets in gas, chloroform, acetic acid, ethanol, DMF, DMSO and water phases.

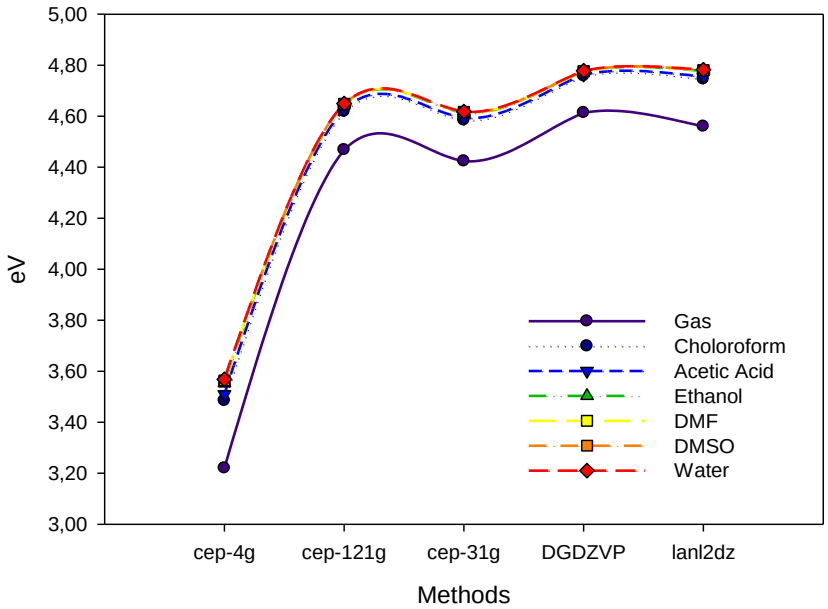

Figure 2. The calculated energy gap (ΔE) parameters by using CEP-4G, CEP-121G, CEP-31G, DGDZVP and LANL2DZ basis sets in gas, chloroform, acetic acid, ethanol, DMF, DMSO and water phases.

Additionally, the, chemical potential, electron affinity, electronegativity chemical hardness, softness and electrophilicity index parameters of iopromide molecule calculated by the DFT level and B3LYP functionals with the CEP-4G, CEP-31G, CEP-121G, DGDZVP and LANL2DZ basis sets in gas phase and chloroform, acetic acid, ethanol, DMF, DMSO and water phases found using the computed E_{HOMO} and E_{LUMO} were summarized in **Table 1**.

Table 1. The calculated quantum chemical parameter values.

Phase	Method	E_{HOMO}, eV	E_{LUMO}, eV	ΔE, eV	η, eV	σ, eV^{-1}	χ, eV	μ, eV	ω, eV	ε, eV	ω, eV	MAC, e	SNPA, e
Gas	B3LYP-CEP-121	-6.971	-2.503	4.468	2.234	0.224	9.475	-9.475	20.093	11.735	30.685	-3.656	-9.400
	B3LYP-CEP-4G	-6.077	-2.857	3.220	1.610	0.311	8.933	-8.933	24.784	16.656	34.522	-3.354	-7.254
	B3LYP-CEP-31	-6.882	-2.459	4.424	2.212	0.226	9.341	-9.341	19.724	11.489	30.170	-3.379	-9.400
	DGDVZ	-6.915	-2.301	4.614	2.307	0.217	9.216	-9.216	18.410	10.347	28.780	-3.128	-9.467
	LANL2DZ	-6.849	-2.289	4.560	2.280	0.219	9.139	-9.139	18.315	10.316	28.593	-3.899	-9.634
Chloroform	B3LYP-CEP-121	-7.098	-2.479	4.619	2.309	0.217	9.577	-9.577	19.859	11.437	30.591	-3.939	-8.842
	B3LYP-CEP-4G	-6.448	-2.964	3.484	1.742	0.287	9.412	-9.412	25.424	16.883	35.708	-3.435	-7.395
	B3LYP-CEP-31	-7.030	-2.446	4.585	2.292	0.218	9.476	-9.476	19.584	11.255	30.207	-3.704	-9.583
	DGDVZ	-7.039	-2.282	4.757	2.379	0.210	9.321	-9.321	18.261	10.130	28.772	-3.143	-9.627
	LANL2DZ	-7.030	-2.285	4.745	2.373	0.211	9.315	-9.315	18.286	10.157	28.788	-4.102	-9.816
Acetic Acid	B3LYP-CEP-121	-7.106	-2.479	4.627	2.314	0.216	9.586	-9.586	19.858	11.429	30.600	-3.961	-8.856
	B3LYP-CEP-4G	-6.481	-2.972	3.509	1.755	0.285	9.452	-9.452	25.460	16.885	35.790	-3.442	-7.406
	B3LYP-CEP-31	-7.039	-2.446	4.593	2.297	0.218	9.484	-9.484	19.583	11.247	30.216	-3.735	-9.598
	DGDVZ	-7.045	-2.282	4.763	2.382	0.210	9.328	-9.328	18.266	10.129	28.785	-3.138	-9.640
	LANL2DZ	-7.041	-2.286	4.755	2.378	0.210	9.327	-9.327	18.295	10.157	28.812	-4.106	-9.830
Ethanol	B3LYP-CEP-121	-7.125	-2.479	4.646	2.323	0.215	9.604	-9.604	19.855	11.412	30.621	-4.020	-8.892
	B3LYP-CEP-4G	-6.547	-2.994	3.554	1.777	0.281	9.541	-9.541	25.618	16.965	36.047	-3.457	-7.431
	B3LYP-CEP-31	-7.062	-2.448	4.614	2.307	0.217	9.510	-9.510	19.601	11.245	30.264	-3.802	-9.634
	DGDVZ	-7.061	-2.285	4.776	2.388	0.209	9.346	-9.346	18.289	10.137	28.828	-3.174	-9.670
	LANL2DZ	-7.067	-2.289	4.777	2.389	0.209	9.356	-9.356	18.323	10.161	28.873	-4.165	-9.865
DMF	B3LYP-CEP-121	-7.127	-2.479	4.648	2.324	0.215	9.606	-9.606	19.855	11.410	30.623	-4.027	-8.896
	B3LYP-CEP-4G	-6.556	-2.996	3.560	1.780	0.281	9.552	-9.552	25.626	16.964	36.068	-3.459	-7.434
	B3LYP-CEP-31	-7.064	-2.448	4.616	2.308	0.217	9.513	-9.513	19.605	11.246	30.272	-3.810	-9.638
	DGDVZ	-7.061	-2.285	4.776	2.388	0.209	9.346	-9.346	18.289	10.136	28.829	-3.166	-9.673
	LANL2DZ	-7.069	-2.290	4.779	2.390	0.209	9.359	-9.359	18.327	10.163	28.881	-4.170	-9.869
DMSO	B3LYP-CEP-121	-7.128	-2.479	4.649	2.324	0.215	9.607	-9.607	19.855	11.410	30.624	-4.030	-8.898
	B3LYP-CEP-4G	-6.560	-2.996	3.564	1.782	0.281	9.556	-9.556	25.626	16.960	36.073	-3.460	-7.435
	B3LYP-CEP-31	-7.065	-2.448	4.617	2.308	0.217	9.514	-9.514	19.605	11.245	30.273	-3.814	-9.639
	DGDVZ	-7.063	-2.286	4.778	2.389	0.209	9.349	-9.349	18.293	10.139	28.836	-3.163	-9.675
	LANL2DZ	-7.070	-2.290	4.781	2.390	0.209	9.360	-9.360	18.327	10.162	28.883	-4.172	-9.870
Water	B3LYP-CEP-121	-7.129	-2.480	4.650	2.325	0.215	9.609	-9.609	19.857	11.410	30.628	-4.034	-8.900
	B3LYP-CEP-4G	-6.566	-2.998	3.568	1.784	0.280	9.563	-9.563	25.632	16.961	36.088	-3.461	-7.437
	B3LYP-CEP-31	-7.067	-2.449	4.618	2.309	0.217	9.516	-9.516	19.607	11.246	30.278	-3.819	-9.642
	DGDVZ	-7.064	-2.286	4.778	2.389	0.209	9.350	-9.350	18.295	10.140	28.840	-3.179	-9.677
	LANL2DZ	-7.072	-2.290	4.782	2.391	0.209	9.362	-9.362	18.330	10.163	28.888	-4.176	-9.873

The hardness (η) of iopromide in the ground state increases in the order; 2.280eV in gas phase < 2.373 eV in chloroform < 2.378 eV in acetic acid < 2.389 eV in ethanol < 2.390 eV in DMF = 2.390 eV in DMSO < 2.391 eV in water at LANL2DZ basis set. The similar trend was found for the other studied basis sets.

The chemical potentials (μ) of iopromide in the ground state increases in the order; gas > chloroform > acetic acid > ethanol> DMF > DMSO> water for LANL2DZ basis set. Therefore, if it is desired to have highest chemical potential, iopromide in the ground state, then out of five solvents studied chloroform is the best, however it is the best in gas phase. The same order is found for the CEP-4G, CEP-31G, CEP-121G and DGDZVP basis sets.

The electrophilicity (ω) of iopromide molecule has been found to possess high electrophilicity in the ground in water, then follow DMF and DMSO solution. The electrophilicity index of iopromide molecule has been found to possess small in the ground in gas phase. Nucleofugality (ε) is the highest in gas phase for studied basis sets.

The electron density of phenyl group was calculated and presented in **Table 2**. As seen of the **Table 2**, negative electron density on the phenyl group means that substituents in the ring increased the available electron density in the ring. It was found that, as electron density in the ring changed in the order; gas > water > DMSO > DMF > ethanol > acetic acid > chloroform for LANL2DZ basis set. The electron density of the ring is found biggest in the gas phase for studied basis sets.

Table 2. Electron density of phenyl group.

Method	Gas	Chloroform	Acetic acid	Ethanol	DMF	DMSO	Water
B3LYP-CEP-121	-0.16482	-0.16345	-0.16316	-0.16357	-0.16362	-0.16367	-0.16369
B3LYP-CEP-31	-0.16028	-0.15914	-0.15934	-0.15969	-0.15975	-0.15977	-0.15981
DGDVZ	-0.16512	-0.15368	-0.15332	-0.15124	-0.15269	-0.15121	-0.15118
LANL2DZ	-0.17452	-0.17172	-0.17185	-0.17228	-0.17233	-0.17235	-0.17238

In the present study the electronic dipole moment, molecular mean polarizability (‹α› determined by considering only the diagonal elements, anisotropy of polarizability (Δα), and Kappa of the title compounds has been calculated using the following expressions (Eq. 9), and shown in **Figure 5**.

$$\alpha = \frac{1}{3}(\alpha_{xx} + \alpha_{yy} + \alpha_{zz})$$

$$\Delta\alpha = \left[\frac{(\alpha_{xx} - \alpha_{yy})^2 + (\alpha_{yy} - \alpha_{zz})^2 + (\alpha_{zz} - \alpha_{xx})^2 + 6(\alpha_{xz}^2 + \alpha_{xy}^2 + \alpha_{yz}^2)}{2}\right]^{1/2}$$

$$k = \frac{(\alpha_{xx}^2 + \alpha_{yy}^2 + \alpha_{zz}^2)}{6<\alpha>^2} \quad (9)$$

Since the values of the polarizabilities (α) and first-order hyperpolarizability (β) of Gaussian 09 output [43] are reported in atomic units (a.u.), the calculated values have been converted into electrostatic units (esu) (α: 1 a.u. = 0.1482 x10^{-24} esu; β: 1 a.u.= 8.6393 x10^{-33} esu) [44].

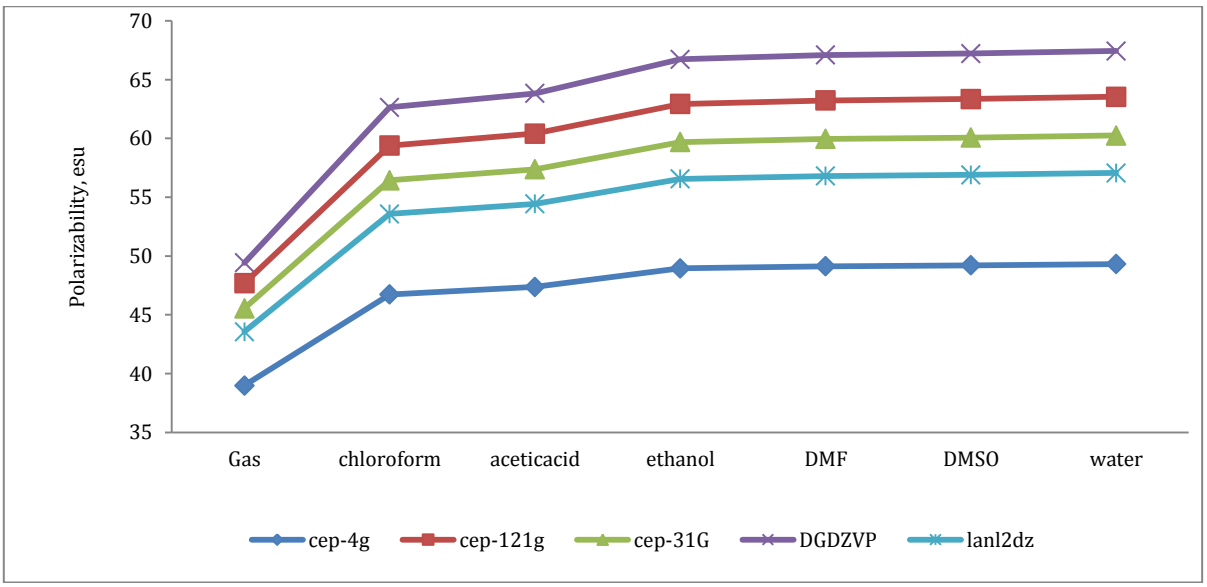

Figure 5. The calculated polarizability values.

In **Figure 6** the comparison between CEP-4G, CEP-31G, CEP-121G, DGDZVP and LANL2DZ basis sets on the calculation of mean polarizability (‹α›), anisotropy of polarizability (Δα) and Kappa was given. Polarizations are the dynamic response of a connected system and gives an idea of the internal structure of a molecule.

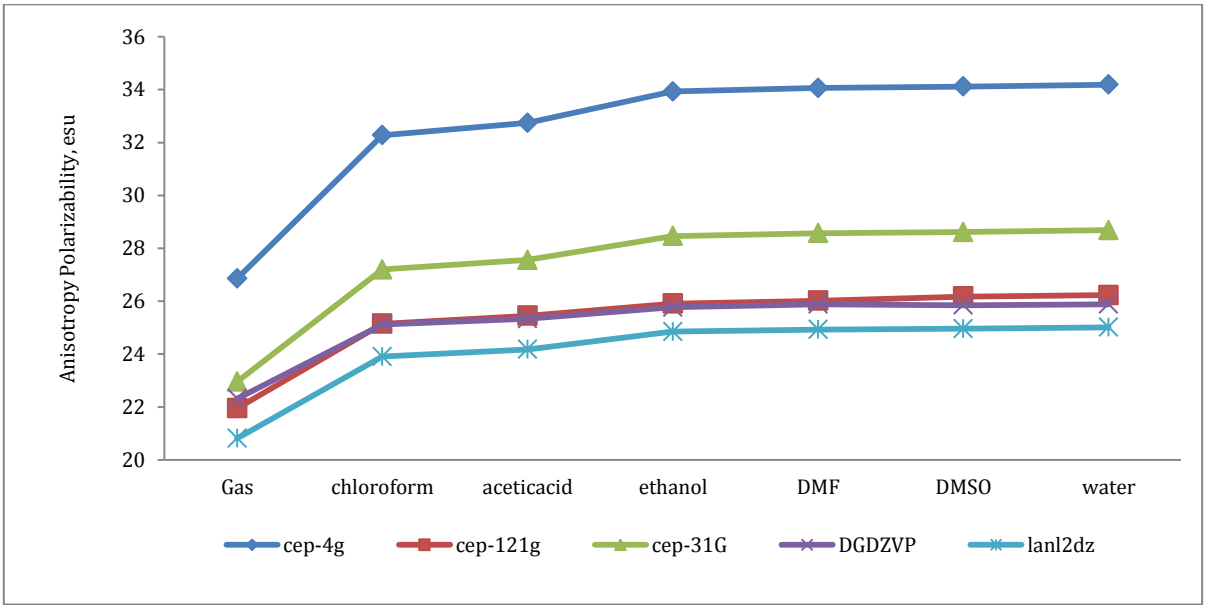

Figure 6. The calculated anisotropy polarizability values.

Polarizability of iopromide calculated by B3LYP/LANL2DZ, changed from 43.56×10^{-24} esu (gas phase), to (chloroform, acetic acid, ethanol, DMF, DMSO and water are 53.57×10^{-24} esu, 54.44×10^{-24} esu, 56.56×10^{-24} esu, 56.80×10^{-24} esu, 56.91×10^{-24} esu, 57.07×10^{-24} esu, respectively). In the same way, polarizabilities calculated with the other basis sets also significantly changed with changing medium polarity.

Increase in the polarizability of iopromide was 21%, 25%, 24%, 27% and 24% for CEP-4G, CEP-31G, CEP-121G, DGDZVP and LANL2DZ basis sets, respectively. Janjua reported that values of polarizability increase were 78%, 121% and 156% for B3LYP, CAM-B3LYP and LC-B3LYP, respectively [45]. Mikkelsen et al. [46] reported that values of polarizability increase about 18% in water solution compared with the gas phase. Bartkowiak and Lipinski reported a 9% increase for the polarizability value in water compared with the gas phase [47].

Anisotropy polarizability of iopromide calculated by B3LYP/LANL2DZ, changed from 20.81×10^{-24} esu (gas phase), to (chloroform, acetic acid, ethanol, DMF, DMSO and water are 23.91×10^{-24} esu, 24.18×10^{-24} esu, 24.85×10^{-24} esu, 24.93×10^{-24} esu, 24.96×10^{-24} esu, 25.01×10^{-24} esu, respectively. In the same way, polarizabilities calculated with the other basis sets also slightly changed with changing medium polarity.

The complete equation for calculating the magnitude of the total first static hyperpolarizability from Gaussian 09 output is given as the equation 10.

$$\beta = \left(\beta_x^2 + \beta_y^2 + \beta_z^2\right)^{1/2}$$

$$\beta = \left[\left(\beta_{xxx} + \beta_{xyy} + \beta_{xzz}\right)^2 + \left(\beta_{yyy} + \beta_{yzz} + \beta_{yxx}\right)^2 + \left(\beta_{zzz} + \beta_{zxx} + \beta_{zyy}\right)^2\right]^{1/2} \quad (10)$$

Since the values of the polarizability α and the first hyperpolarizability β of Gaussian 09 output are reported in atomic units (a.u.), the calculated values have been converted into electrostatic units (esu) (β: 1 a.u. = 8.6393×10^{-33} esu). **Table 3** listed B3LYP method with the CEP-4G, CEP-31G, CEP-121G, LANL2DZ basis sets in gas phase and different solvents such as chloroform, acetic acid, ethanol, results of the first hyperpolarizability β for iopromide. The highest value of first hyperpolarisibility is calculated by Cep-4G basis set is equal to 4.64×10^{-30} esu. The calculated first hyperpolarizability β by LANL2DZ, CEP-4G, CEP-31G, CEP-121G and DGDZVP basis sets are equal to 2.94×10^{-30} esu, 4.43×10^{-30} esu, 3.10×10^{-30} esu, 3.99×10^{-30} esu and 3.18×10^{-30} esu, respectively.

Table 3. First hyperpolarizability β for iopromide as values $\times10^{-30}$.

Phase	LANL2DZ	Cep-4G	Cep-31G	CEP-121	DGDZVP
Gas	2.94	4.43	3.10	3.99	3.18
Chloroform	3.07	4.55	3.21	3.95	3.95
Acetic acid	3.05	4.56	3.06	3.99	4.00
Ethanol	2.96	4.62	2.84	3.85	4.22
DMF	2.95	4.63	2.96	3.83	4.11
DMSO	2.94	4.64	2.95	3.82	4.21
Water	2.93	4.64	2.77	3.80	4.21

The standard statistical thermodynamic functions such as heat capacity, entropy and enthalpy changes for iopromide in gas and solvent phase (chloroform, acetic acid, ethanol, DMF, DMSO and water) were obtained from the theoretical harmonic frequencies on the basis of vibrational analysis at B3LYP/LANL2DZ level and presented in **Figure 7**.

Thermodynamic parameters in gas and solvent media were found to be varied with varying temperature. The computed values of heat capacity were observed to increase with the increasing temperature. The value of heat capacity was found at 200 K as 94 cal/mol; at 500 K as 174 cal/mol; and at 1000 K as 239 cal/mol. The similar trend was found for the solvent media. The value of heat capacity is the smallest in gas phase for the all temperatures studied except 200 K. And at the temperature between 230 K and 1000 K heat capacity value increase from ongoing gas phase to the water phase. The computed values of entropy and corrected enthalpy were observed to increase with the increasing temperature in gas phase and solvent media studied due to the fact that main contributions to the thermodynamic functions are from the translations and rotations of molecules at a lower temperature, however, the vibrations in the high temperature contribute more to their thermodynamic functions the molecular vibrational intensities increase with temperature [48].

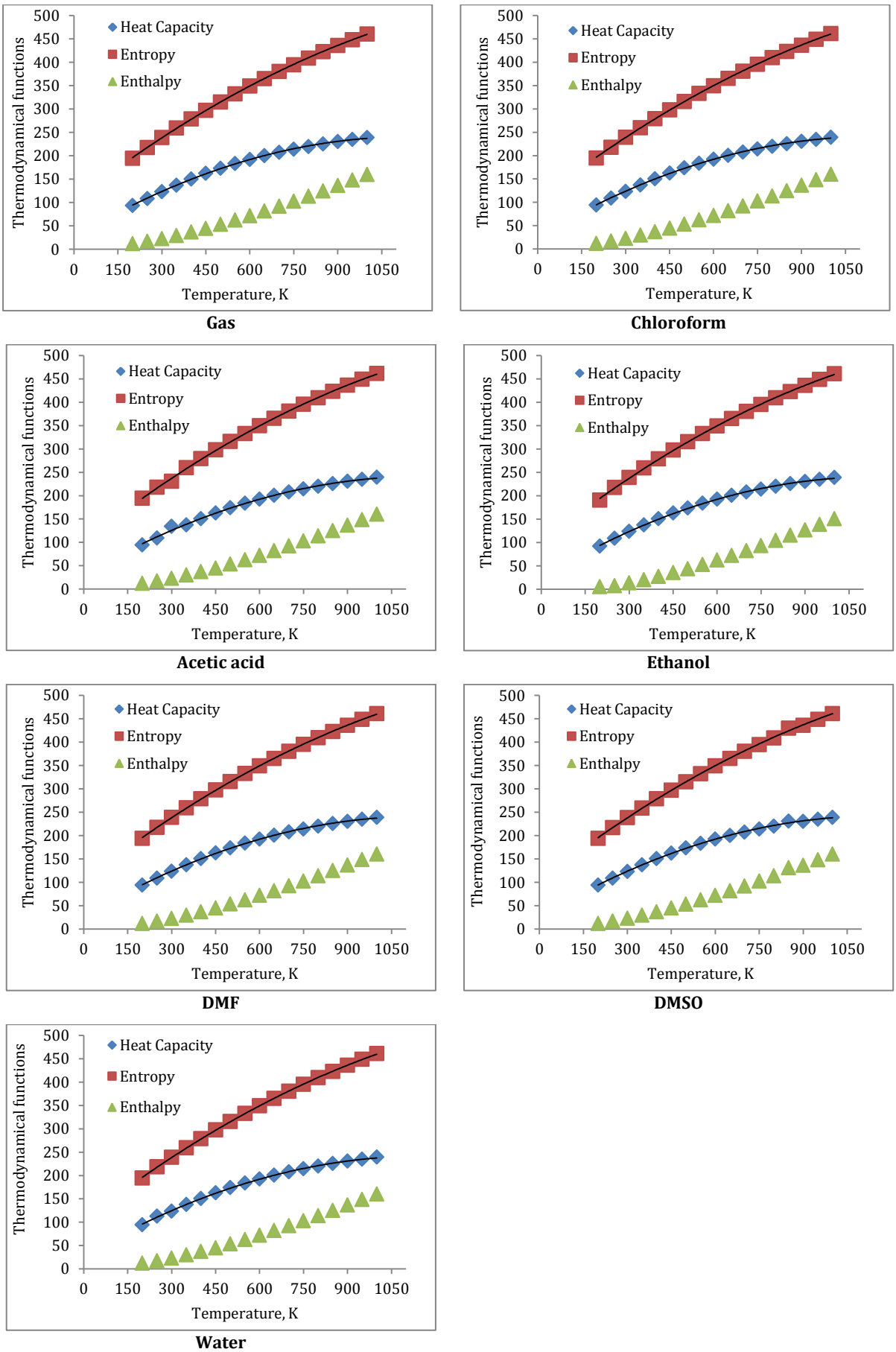

Figure 7. Thermodynamic properties at different temperatures at the B3LYP/LANL2DZ level of iopromide.

The correlation equations between temperatures and heat capacities, entropies, enthalpy were fitted by quadratic formulas, and the corresponding fitting factors (R^2) for heat capacity entropy and enthalpy are 0.9998,

0.99999 and 0.9998, respectively, and the corresponding fitting equations for these thermodynamic functions for gas phase are $C = -0.0002T^2 + 0.3808T + 24.649$, $S = -0.0001T^2 + 0.4893T + 103.66$ and $H = 9E\text{-}05T^2 + 0.0821T + 90876$.

Fitting equations for heat capacity entropy and enthalpy and correlation coefficient in solvent media are given in **Table 4**.

Table 4. Equation and Correlation coefficient between temperatures and heat capacities, entropies, enthalpy.

Media	Heat Capacity	Entropy	Enthalpy
Gas	$C = -0.0002T^2 + 0.3808T + 24.649$ $R^2 = 0.9998$	$S = -0.0001T^2 + 0.4893T + 103.660$ $R^2 = 0.9999$	$H = 9E\text{-}05T^2 + 0.0821T + 9.0876$ $R^2 = 0.9998$
Chloroform	$C = -0.0002T^2 + 0.3739T + 26.421$ $R^2 = 0.9996$	$S = -0.0001T^2 + 0.4904T + 103.730$ $R^2 = 0.9999$	$H = 9E\text{-}05T^2 + 0.0824T - 9.1085$ $R^2 = 0.9998$
Acetic acid	$C = -0.0002T^2 + 0.3629T + 30.880$ $R^2 = 0.9971$	$S = -0.0001T^2 + 0.4992T + 99.977$ $R^2 = 0.9995$	$H = 9E\text{-}05T^2 + 0.0828T - 9.2518$ $R^2 = 0.9998$
Ethanol	$C = -0.0002T^2 + 0.3807T + 24.301$ $R^2 = 0.9995$	$S = -0.0001T^2 + 0.5008T + 99.927$ $R^2 = 0.9998$	$H = 1E\text{-}04T^2 + 0.0729T - 15.976$ $R^2 = 0.9994$
DMF	$C = -0.0002T^2 + 0.3801T + 25.143$ $R^2 = 0.9998$	$S = -0.0001T^2 + 0.4906T + 103.140$ $R^2 = 0.9999$	$H = 9E\text{-}05T^2 + 0.0828T - 9.2518$ $R^2 = 0.9998$
DMSO	$C = -0.0002T^2 + 0.3749T + 26.055$ $R^2 = 0.9992$	$S = -0.0001T^2 + 0.4919T + 102.610$ $R^2 = 0.9996$	$H = 9E\text{-}05T^2 + 0.0836T - 9.5952$ $R^2 = 0.9986$
Water	$C = -0.0002T^2 + 0.3721T + 27.819$ $R^2 = 0.9996$	$S = -0.0001T^2 + 0.4889T + 103.720$ $R^2 = 0.9999$	$H = 9E\text{-}05T^2 + 0{,}0828T - 9.2518$ $R^2 = 0.9988$

All thermodynamic calculations were done in gas phase and chloroform, acetic acid, ethanol, DMF, DMSO and water media. These data supply helpful information for the further study on the iopromide.

4. Conclusion

In the present work, we have performed density functional theory calculations B3LYP method with the CEP-4G, CEP-31G, CEP-121G, DGDZVP, LANL2DZ basis sets in gas and other solvent phases, and solution electronic properties iopromide. Molecular properties such E_{HOMO}, E_{LUMO}, global hardness, chemical potential, global electrophilicity, nucleofugality and electrofugality were calculated. Solvent ability in engaging to structure of the compound can influence energy levels as well as HOMO or LUMO levels, and the parameters related with HOMO and LUMO energies.

In addition to thermodynamic properties of this molecule was calculated B3LYP/LANL2DZ method for gas and solvent media. The correlations between the statistical thermodynamics and temperature were obtained. It is seen that the heat capacities, entropies and enthalpies increase with the increasing temperature due to intensities of the molecular vibrations increase with increasing temperature.

References

[1] Almén, T. 1994. The etiology of contrast medium reactions. Invest Radiol; 29 Suppl. 1, 37-45.

[2] Stacul, F. 2001. Current iodinated contrast media. Eur. Radiol. 11, 690-697.

[3] Kooiman, J., Pasha, S. M., Zondag, W., et al. 2011. Meta-analysis: serum creatinine changes following contrast enhanced CT imaging, Eur. J. Radiol., 81, 2554–2561.

[4] Seong, J. M., Choi, N. M., Lee, J. Y., Chang, Y., Kim, Y., Yang, B. R., Jin, X. M., Kim, J. Y., Park, B. J. 2013. Comparison of the Safety of Seven Iodinated Contrast Media. Korean Med Sci. 28: 1703-1710.

[5] Zhejiang, S. 2012. Synthesis of Iopromide, Chinese Journal of Pharmaceuticals. 43, I7, 527-529

[6] Frisch, M. J.; Trucks, G. W.; Schlegel, H. B.; Scuseria, G. E.; Robb, M. A.; Cheeseman, J. R.; Scalmani, G.; Barone, V.; Mennucci, B.; Petersson, G. A.; Nakatsuji, H.; Caricato, M.; Li, X.; Hratchian, H. P.; Izmaylov, A. F.; Bloino, J.; Zheng, G.; Sonnenberg, J. L.; Hada, M.; Ehara, M.; Toyota, K.; Fukuda, R.; Hasegawa, J.; Ishida, M.; Nakajima, T.; Honda, Y.; Kitao, O.; Nakai, H.; Vreven, T.; Montgomery, J. A., Jr.; Peralta, J. E.; Ogliaro, F.; Bearpark, M.; Heyd, J. J.; Brothers, E.; Kudin, K. N.; Staroverov, V. N.; Kobayashi, R.; Normand, J.; Raghavachari, K.; Rendell, A.; Burant, J. C.; Iyengar, S. S.; Tomasi, J.; Cossi, M.; Rega, N.; Millam, J. M.; Klene, M.; Knox, J. E.; Cross, J. B.; Bakken, V.; Adamo, C.; Jaramillo, J.; Gomperts, R.; Stratmann, R. E.; Yazyev, O.; Austin, A. J.; Cammi, R.; Pomelli, C.; Ochterski, J. W.; Martin, R. L.; Morokuma, K.; Zakrzewski, V. G.; Voth, G. A.; Salvador, P.; Dannenberg, J. J.; Dapprich, S.; Daniels, A. D.; Farkas, Ö.; Foresman, J. B.; Ortiz, J. V.; Cioslowski, J.; Fox, D. J. Gaussian, Inc., Wallingford CT, 2009.

[7] Dennington II R. D.; Keith T.A.; Millam J.M. 2009. GaussView 5.0, Wallingford, CT.

[8] Stephens, P. J., Devlin, F. J., Chabalowski, C. F., Frisch, M. J. 1994. Ab Initio Calculation of Vibrational Absorption and Circular Dichroism Spectra Using Density Functional Force Fields. J. Phys. Chem. 98, 11623-11627.

[9] Ozimiński, W. P., Garnuszek, P., Bednarek, E., Cz Dobrowolski, J. 2007. The platinum complexes with histamine: Pt(II)(Hist)Cl_2, Pt(II)(Iodo-Hist)Cl_2 and Pt(IV)(Hist)2Cl_2. Inorg. Chim. Acta. 360, 1902-1914.

[10] Stevens, W. J., Basch, H., Krauss, M. 1984. Compact effective potentials and efficient shared-exponent basis-sets for the 1st-row and 2nd-row atoms, J. Chem. Phys., 81, 6026-6023.

[11] Gao, H. 2011. Theoretical studies of molecular structures and properties of platinum (II) antitumor drugs. Spectrochimica Acta - Part A: Molecular and Biomolecular Spectroscopy. 79, 687-693.

[12] Kaya, S., Kaya, C., Guo, L., Kandemirli, F., Tüzün, B., Uğurlu, İ., Madkour, L. H., Saracoglu, M. 2016. Quantum chemical and molecular dynamics simulation studies on inhibition performances of some thiazole and thiadiazole derivatives against corrosion of iron, J. Mol. Liq., 219, 497-504.

[13] Ebenso, E. E., Arslan, T., Kandemirli, F., Love, I., Öğretir, C., Saracoglu, M., Umoren, S. A. 2010. Theoretical studies of some sulphonamides as corrosion inhibitors for mild steel in acidic medium, Int. J. Quantum Chem., 110, 2614-2636.

[14] Amin, M. A., Ahmed, M. A., Arida, H. A., Arslan, T., Saracoglu, M., Kandemirli, F. 2011. Monitoring corrosion and corrosion control of iron in HCl by non-ionic surfactants of the TRITON-X series-Part II. Temperature effect, activation energies and thermodynamics of adsorption, Corros. Sci., 53, 540-548.

[15] Amin, M. A., Ahmed, M. A., Arida, H. A., Kandemirli, F., Saracoglu, M., Arslan, T., Basaran, M. A. 2011. Monitoring corrosion and corrosion control of iron in HCl by non-ionic surfactants of the TRITON-X series-Part III. Immersion time effects and theoretical studies, Corros. Sci., 53, 1895-1909.

[16] Zor, S., Saracoglu, M., Kandemirli, F., Arslan, T. 2011. Inhibition effects of amides on the corrosion of copper in 1.0 M HCl: Theoretical and experimental studies, Corrosion, **67**, 12, 125003-1-125003-11 (11 pages).

[17] Kandemirli, F., Saracoglu, M., Bulut, G., Ebenso, E., Arslan, T., Kayan, A. 2012. Synthesis and theoretical study of zinc(II) and nickel(II) complexes of 5-methoxyisatin 3-[N-(4-chlorophenyl)thiosemicarbazone], ITB J. Science (J. Math. and Fund. Sci.), 44A, 35-50.

[18] Amin, M. A., Hazzazi, O. A., Kandemirli, F., Saracoglu, M. 2012. Inhibition performance and adsorptive behaviour of three amino acids on cold rolled steel in 1.0 M HCl-chemical, electrochemical and morphological studies, Corrosion, 68, 688-698.

[19] Kandemirli, F., Saracoglu, M., Amin, M. A., Basaran, M. A., Vurdu, C. D. 2014. The Quantum chemical calculations of serine, therionine and glutamine, Int. J. Electrochem. Sci., 9, 3819-3827.

[20] Amin, M. A., El-Bagoury, N., Saracoglu, M., Ramadan, M. 2014. Electrochemical and corrosion behavior of cast re-containing inconel 718 alloys in sulphuric acid solutions and the effect of Cl^-, Int. J. Electrochem. Sci., 9, 5352-5374.

[21] Kandemirli, F., Vurdu, C. D., Saracoglu, M., Akkaya, Y.Cavus, M. S. 2015. Some molecular properties and reaction mechanism of synthesized isatin thiosemicarbazone and its zinc(II) and nickel(II) complexes, Int. Res. J. Pure and Applied Chem., 9, 1-16.

[22] El-Bagoury, N., Amin, M. A., Saracoglu, M. 2015. Effect of aging treatment on the electrochemical and corrosion behavior of nitire shape memory alloy, Int. J. Electrochem. Sci., 10, 5291-5308.

[23] İlhan, İ. Ö., Çadır, M., Saracoglu, M., Kandemirli, F., Kökbudak, Z., Akkoç, S. 2015. The reactions and quantum chemical calculations of some pyrazole-3-carboxylic acid chlorides with various hydrazides, Chem. Sci. Rev. Lett., 4, 838-850.

[24] Amin, M. A., Fadlallah, S. A., Alosaimi, G. S., Kandemirli, F., Saracoglu, M., Szunerits, S., Boukherroub, R. 2016. Cathodic activation of titanium-supported gold nanoparticles: an efficient and stable electrocatalyst for the hydrogen evolution reaction, Int. J. Hyd. Energy, 41, 6326-6341.

[25] Tazouti, A., Galai, M., Touir, R., Ebn Touhami, M., Zarrouk, A., Ramli, Y., Saraçoğlu, M., Kaya, S., Kandemirli, F., Kaya, C. 2016. Experimental and theoretical studies for mild steel corrosion inhibition in 1 M HCl by three new quinoxalinone derivatives, J. Mol. Liquids, 221, 815-832.

[26] Amin, M. A., Saracoglu, M., El-Bagoury, N., Sharshar, T., Ibrahim, M. M., Wysocka, J., Krakowiak, S., Ryl, J. 2016. Microstructure and corrosion behaviour of carbon steel and ferritic and austenitic stainless steels in NaCl solutions and the effect of p-Nitrophenyl phosphate disodium salt, Int. J. Electrochem. Sci., 11, 10029-10052.

[27] Saracoglu, M., Kandemirli, F., Ozalp, A., Kokbudak, Z. 2017. Synthesis and quantum chemical calculations of 2,4-dioxopentanoic acid derivatives-Part I, Chem. Sci. Rev. Lett., 6, 1-11.

[28] Saracoglu, M., Kandemirli, F., Ozalp, A., Kokbudak, Z. 2017. Synthesis and quantum chemical calculations of 2,4-dioxopentanoic acid derivatives-part II, Int. J. Sci. Eng. Inv., 6, 50-57.

[29] Saima, B., Khan, A., Un Nisa, R., Mahmood, T., Ayub, K. 2016. Theoretical insights into thermal cyclophanediene to dihydropyrene electrocyclic reactions; a comparative study of Woodward Hoffmann allowed and forbidden reactions, J. Mol. Model., 22, 81 (9 pages).

[30] Saracoglu, M., Elusta, M. I. A., Kaya, S., Kaya, C., Kandemirli, F. 2018. Quantum chemical studies on the corrosion inhibition of $Fe_{78}B_{13}Si_9$ glassy alloy in Na_2SO_4 solution of some thiosemicarbazone derivatives, Int. J. Electrochem. Sci., 13, 8241-8259.

[31] Saracoglu, M., Kokbudak, Z., Çimen, Z., Kandemirli, F. 2019. Synthesis and DFT Quantum Chemical Calculations of Novel Pyrazolo[1,5-c]pyrimidin-7(1H)-one Derivatives, J. Chem. Soc. Pak., 41, 5-841-858.

[32] Saracoglu, M., Kandemirli, S.G., Başaran, A., Sayiner, H., Kandemirli, F. 2011. Investigation of structure-activity relationship between chemical structure and CCR5 anti HIV-1 activity in a class of 1-[N-(methyl)-N-(phenylsulfonyl)amino]-2-(phenyl)-4-[4-(substituted)piperidin-1-yl] butanes derivatives: The electronic-topological approach, Curr. HIV Res., 9, 300-312.

[33] Saracoglu, M., Kandemirli, F., Amin, M. A., Vurdu, C. D., Cavus, M. S., Sayıner, G. 2015. The quantum chemical calculations of some thiazole derivatives, Proceedings of the 3rd International Conference on Computation for Science and Technology (ICCST-3), Published by Atlantis Press, 5, 149-154.

[34] Khaled, K. F. 2010. Studies of iron corrosion inhibition using chemical, electrochemical and computer simulation techniques, Electrochim. Acta, 55, 6523-6532.

[35] Dewar, M. J., Thiel, W. 1977. Ground states of molecules. 38. The MNDO method. Approximations and parameters, J. Am. Chem. Soc., 99, 4899-4907.

[36] Pearson, R. G. 1990. Hard and soft acids and bases-the evolution of a chemical concept, Coord. Chem. Rev., 100, 403-425.

[37] Pauling, L. 1960. The Nature of the Chemical Bond, Cornell University Press, Ithaca, New York.

[38] Parr, R. G., Pearson, R.G. 1983. Absolute hardness: companion parameter to absolute electronegativity, J. Am. Chem. Soc., 105, 7512-7516.

[39] Chattaraj, P. K., Sarkar, U., Roy, D.R. 2006. Electrophilicity index, Chem. Rev., 106, 2065-2091.

[40] Ebenso, E. E., Kabanda, M. M., Arslan, T., Saracoglu, M., Kandemirli, F., Murulana, L. C., Singh, A. K., Shukla, S. K., Hammouti, B., Khaled, K. F., Quraishi, M. A., Obot, I. B., Edd, N. O. 2012. Quantum chemical investigations on quinoline derivatives as effective corrosion inhibitors for mild steel in acidic medium, Int. J. Electrochem. Sci., 7, 5643-5676.

[41] Ding L, Ying H, Zhou Y, Lei T, Pei J. 2010. Polycyclic imide derivatives: Synthesis and effective tuning of lowest unoccupied molecular orbital levels through molecular engineering, Org. Lett. 12(23), 5522-5525.

[42] Abbaz, T., Benjeddou, A., Villemin, D. 2018. Molecular structure, HOMO, LUMO, MEP, Natural bond orbital analysis of benzo and Anthraquinodimethane Derivatives. Pharmaceutical and Biological Evaluations 5(2) 27-39.

[43] Krishnan, R., Binkley, J. S., Seeger, R., et al. 1980. Self-consistent molecular orbital methods. XX. A basis set for correlated wave functions, Journal of Chemical Physics, 72, 650-655.

[44] Ben Ahmed, A., Feki, H., Abid, Y., Boughzala, H., Mlayah, A. 2008. Structural, vibrational and theoretical studies of l-histidine bromide, J. Mol. Struct., 888, 1-3, 180-186.

[45] Janjua, M. R. S. A., Mahmood, A., Ahmad, F. 2013. Solvent effects on nonlinear optical response of certain tetramminеruthenium (II) complexes of modified 1,10-phenanthrolines, Can. J. Chem., Vol. 91 (12), 1303-1309

[46] Mikkelsen, K. V.; Luo, Y.; Agren, H.; Jùrgensen, P. J. 1994. Solvent induced polarizabilities and hyperpolarizabilities of para-nitroaniline studied by reaction field linear response theory J. Chem. Phys., 100, 8240-8250.

[47] Bartkowiak, W.; Lipinski, J. 1998. Solvent effect on the nonlinear optical properties of para-nitroaniline studied by Langevin dipoles–Monte Carlo (LD/MC) approach, Comput. Chem. 22 (1), 31-37.

[48] Govindarajan, M., Karabacak, M. 2012. FT-IR, FT-Raman and UV spectral investigation; computed frequency estimation, analysis and electronic structure calculations on 1-nitronaphthalene, Spectrochimica Acta Part A, 85, 251–260.